Nanoparticles

DOI: 10.1002/anie.201001213

Colloidal Synthesis of Non-Equilibrium Wurtzite-Type MnSe**

*Ian T. Sines, Rajiv Misra, Peter Schiffer, and Raymond E. Schaak**

Manganese chalcogenides exhibit a variety of important magneto-optical properties that collectively result from their crystal structures, the large number of unpaired electrons in high-spin Mn^{2+}, bandgaps that span visible to ultraviolet wavelengths, and interesting magnetic ordering schemes.[1] In particular, manganese selenide (MnSe) is an intensively studied antiferromagnetic semiconductor with interesting magnetic ordering behavior, especially as a component in thin-film superlattices where the type of magnetic ordering can be tuned with strain, dimensionality, and film thickness.[2] Solid solutions of manganese-doped ZnSe, for example, permit tuning of the coupled electronic, optical, and magnetic properties,[3] and MnSe is the $x = 1$ end member of the solid solution of the magnetic semiconductor $Zn_{1-x}Mn_xSe$.[4] MnSe is most stable in the octahedrally coordinated rocksalt (RS) structure type,[5] and a number of studies have focused on the synthesis and properties of this polymorph as bulk powders,[6] thin films,[7] and nanostructured solids.[8] The tetrahedrally coordinated non-equilibrium zincblende (ZB) and wurtzite (WZ) polymorphs are extremely rare, yet are of interest because of their direct structural compatibility with III/V, II/VI, and related semiconductor systems. It has been reported that $Zn_{1-x}Mn_xSe$ adopts the ZB structure for $0 < x < 0.30$ and the WZ structure for $0.30 < x < 0.57$.[3] ZB-type MnSe has been stabilized as epitaxial films on ZB-type ZnSe and GaAs substrates,[9] and impure powders have been made by a gas-phase precipitation reaction.[10] WZ-type MnSe is known to be highly unstable,[5] and has only been observed as minor impurity phases.[10] The inability to isolate nominally phase-pure, bulk-scale quantities of the non-equilibrium tetrahedrally bonded polymorphs of MnSe, particularly the elusive WZ polymorph, precludes some detailed studies of their properties and structures and represents a significant gap in this important family of magnetic semiconductors.

Herein we report a colloidal synthesis route to WZ-type MnSe (γ-MnSe), which forms as solution-dispersible nanoparticles. This result represents the first example of the tetrahedrally bonded WZ-type MnSe polymorph that is accessible in sufficient quantities to characterize the optical and magnetic properties, and complements theoretical and thin-film investigations of this and related materials that have been carried out over the past few decades.[4,11]

In a typical synthesis, WZ-type MnSe was accessed by combining $MnCl_2 \cdot 4H_2O$ (310 mg), Se powder (80 mg), oleic acid (OA, 15 mL), and tetraethylene glycol (TEG, 15 mL) in a three neck flask and heating under Ar to 235 °C over one hour. The sample was maintained at this temperature for 4 hours before cooling to room temperature, washing the precipitate with ethanol, and drying under vacuum. Small amounts of residual Se, when observed, were removed by washing with dilute trioctylphosphine. Oleic acid was required to generate WZ-type MnSe, with a 50:50 ratio of OA/TEG required for phase-pure WZ MnSe. Modifying this mixture with other solvents or stabilizers resulted in the predominant formation of either RS-type MnSe or $MnSe_2$.

Figure 1 shows powder X-ray diffraction (XRD) data for WZ-type MnSe. The pattern matches that expected for the WZ structure type (a hexagonal cell with $a = 4.178(5)$ Å and $c = 6.783(2)$ Å). This compares favorably with the cell parameters previously predicted for WZ-type MnSe by extrapolating known cell constants for $Zn_{1-x}Mn_xSe$ solid solutions ($a_{est} = 4.17$ Å, $c_{est} = 6.81$ Å).[3] Quantitative analysis of the XRD data indicates that more than 85% of the sample consists of WZ-type MnSe. The remainder corresponds to the ZB polymorph, which has an XRD pattern that overlaps with that of WZ MnSe and effectively adds intensity to the 002, 110, and 112 peaks of WZ-type MnSe. The ZB impurity may be present as intergrowths in the WZ structure or as separate particles. Trace amounts of a $MnSe_2$ impurity phase are sometimes present as well, with the most intense peak of $MnSe_2$ appearing as a small bump above the baseline near $2\theta = 31.2°$.

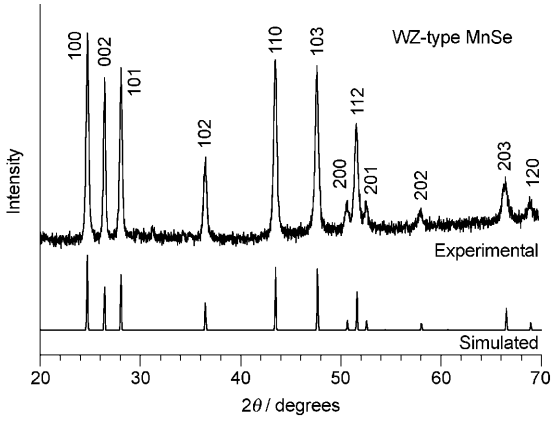

Figure 1. Experimental and simulated powder XRD data for WZ-type MnSe nanoparticles.

[*] I. T. Sines, Prof. R. E. Schaak
Department of Chemistry and Materials Research Institute
The Pennsylvania State University
University Park, PA 16802 (USA)
E-mail: schaak@chem.psu.edu
Dr. R. Misra, Prof. P. Schiffer
Department of Physics and Materials Research Institute
The Pennsylvania State University
University Park, PA 16802 (USA)

[**] This work was supported by the U.S. Department of Energy (DE-FG02-08ER46483), with additional support from a DuPont Young Professor Grant and a Camille Dreyfus Teacher-Scholar Award. R.M. and P.S. thank the Penn State MRSEC (DMR-0820404) and NSF (DMR-0701582) for funding. The TEM imaging was performed in the Electron Microscopy Facility of the Huck Institutes of the Life Sciences. We thank N. Samarth for helpful discussions.

A representative transmission electron microscope (TEM) image of WZ-type MnSe is shown in Figure 2. The product consists of nanoscopic particles that range in size from 25–75 nm and have shapes that are largely isotropic and

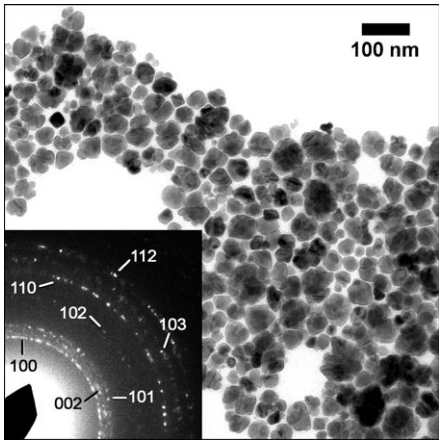

Figure 2. Representative TEM image of WZ-type MnSe nanoparticles. Inset: Corresponding selected area electron diffraction (SAED) pattern.

irregular. The electron diffraction pattern (Figure 2, inset), which clearly shows the 100, 002, 101, 102, and 103 reflections that are characteristic of the hexagonal WZ structure type, confirms that these particles are the WZ polymorph. Energy-dispersive X-ray analysis (not shown) confirms the MnSe stoichiometry ($Mn_{47}Se_{53}$), within experimental error.

Figure 3 shows UV/visible absorption data for WZ-type MnSe nanoparticles dispersed in ethanol. A prominent absorption edge around 350 nm characterizes the UV region, with no observable features present at visible wavelengths. Based on the UV/vis data, the optical band gap (E_g) was estimated to be approximately 3.5–3.8 eV. This value is significantly larger than that for RS-type MnSe ($E_g \approx 2.5$ eV),[12] but is consistent with the band gaps of comparable tetrahedrally coordinated manganese chalcogenides, including ZB-type MnSe ($E_g = 3.4$ eV)[13] and WZ-type MnS ($E_g = 3.8$–3.9 eV).[14]

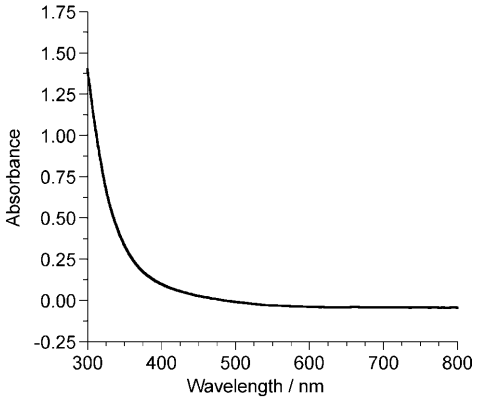

Figure 3. UV/visible absorption spectrum for WZ-type MnSe nanoparticles.

Magnetization measurements taken at 100 Oe (Figure 4) show paramagnetic behavior with an effective moment per Mn atom in the range of 6.0–6.5 μ_B, which compares favorably with the theoretical value of 5.92 μ_B for Mn^{2+} and the reported

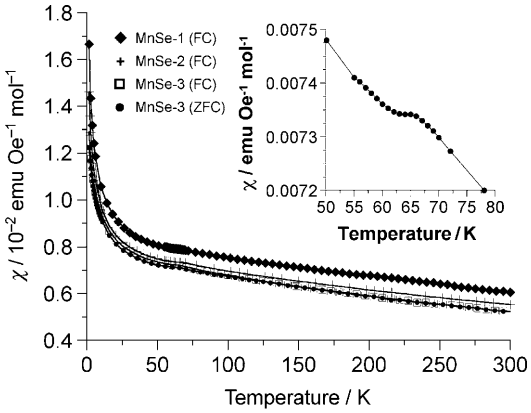

Figure 4. Temperature-dependent magnetic susceptibility (100 Oe) for three samples of WZ-type MnSe. Both FC and ZFC data are shown for one of the samples. The small peak around 64 K, suggestive of antiferromagnetic ordering and present in all samples, is resolved in the inset for a representative sample.

value of 5.88 μ_B for RS-type MnSe.[15] For multiple samples, the data in the range of 200–300 K obey the Curie–Weiss law and gave a Weiss temperature (θ_W) of (-625 ± 50) K. This result indicates strong antiferromagnetic interactions and is consistent with the θ_W values reported for other manganese chalcogenides.[1] All samples that were measured show a small peak around $T = 64$ K (Figure 4, inset), and this peak remained unchanged during field-cooled (FC) and zero-field-cooled (ZFC) measurements. Taken together, the data suggest that most of the Mn moments do not order, presumably because of the small size of the nanoparticles, but that some of the moments order antiferromagnetically with $T_N = 64$ K. This Néel temperature would not correspond to any known $MnSe_x$ or MnO_x phases that could be possible impurities (e.g. $MnSe_2$, MnO), or to RS-type MnSe ($T_N = 150$ K),[8b] so is most likely intrinsic to WZ-type MnSe. Theory predicts that ZB-type MnSe will have $T_N = 90$ K,[11] and experiments have shown Néel temperatures that decrease from 115 K to 75 K in epitaxial films of ZB-type MnSe as the thickness decreases from 6 nm to 0.9 nm.[2] The 64 K feature is unlikely to be associated with a size-induced suppression of T_N in the small fraction of ZB-type MnSe in our samples. This is because the feature is sharp and reproducible and our samples contain a fairly wide range of particle sizes that are, on average, significantly larger than those for which size-dependent phenomena have been previously observed.[2] On the other hand, it is known experimentally that the Néel temperatures for WZ polymorphs are lower than those of their ZB analogues.[1] Therefore, associating the 64 K feature with an antiferromagnetic T_N for WZ-type MnSe would be consistent with this empirical tendency.

In conclusion, WZ-type MnSe (γ-MnSe), a non-equilibrium polymorph of the widely studied MnSe magnetic

semiconductor and an elusive $x = 1$ end member of the solid solution of the magnetic semiconductor $Zn_{1-x}Mn_xSe$, has been synthesized for the first time in isolatable quantities as nanoparticles using a solution chemistry technique. The γ-MnSe nanoparticles have an optical band gap of approximately 3.5–3.8 eV and are largely paramagnetic, with evidence of antiferromagnetic ordering at $T_N = 64$ K.

Experimental Section

Synthesis of WZ-type MnSe: 310 mg of $MnCl_2 \cdot 4H_2O$ (99%, Alfa Aesar), 80 mg of Se powder (99+%, Alfa Aesar), 15 mL oleic acid (OA, 90%, Alfa Aesar), and 15 mL tetraethylene glycol (TEG, 99%, Alfa Aesar) were placed in a three-neck flask, which was sealed using a condenser with an air-flow adapter, a thermometer adapter, and a rubber septum. The three-neck flask was then attached to a Schlenk line and placed under vacuum for 30 min. The three-neck flask was then placed under Ar and heated to 200 °C. The solution was heated at reflux (200 °C), and the vessel was purged by inserting a needle into the septum. The reaction was then heated to 235 °C at which point the solution became a cloudy orange color. The purging needle was then removed and the reaction was held at 235 °C for 4 h. The reaction was then cooled to room temperature. The precipitate was isolated using an equal volume of ethanol and centrifuging for 10 min at 12000 rpm. The supernatant was decanted and the product was washed three times with ethanol before drying under vacuum. If residual selenium was detected, the powder was sonicated in a solution containing 10 drops of trioctylphosphine (TOP) and 1.5 mL hexanes, followed by centrifugation, washing with hexanes and ethanol, and drying under vacuum. Comparative studies were performed by changing the composition of the solvent. γ-MnSe could only be synthesized when oleic acid was present. If TEG was replaced with oleylamine, a mixture of RS- and WZ-type MnSe was formed. If TOP was present, then no MnSe was synthesized. To generate γ-MnSe, it was determined that 50% of the solvent volume must consist of oleic acid. When using less than 50%, $MnSe_2$ was generated.

Characterization of the materials: Powder XRD data were collected on a Bruker Advance D8 X-ray diffractometer using $Cu_{K\alpha}$ radiation. Quantification of WZ:ZB phase fractions was performed by overlaying simulated XRD patterns for WZ-type MnSe and ZB-type MnSe using CrystalDiffract and adjusting the percent composition until the intensities of the simulated pattern matched that of the experimental pattern. The TEM images and SAED patterns were collected using a JEOL JEM 1200 EXII microscope operating at 80 kV. Samples for TEM imaging were deposited from solution onto a carbon-coated Cu TEM grid. Magnetic characterization was performed using a Quantum Design SQUID magnetometer. Energy dispersive X-ray spectroscopy was performed on a FEI Quanta 200 environmental scanning electron microscope operating in high vacuum mode and using a JEOL JSM 5400 scanning electron microscope. UV/visible absorption data were collected using an Ocean Optics HR4000 high-resolution spectrometer with a Micropack DH-2000 BAL UV-Vis NIR light source. Nanoparticle samples were diluted with ethanol for collection of UV/vis data. A control reaction, performed by heating the solvent and stabilizers using the same temperature profile as the reaction used to make WZ-type MnSe, was used as the background for the UV/visible absorption measurement.

Received: February 28, 2010
Published online: May 17, 2010

Keywords: chalcogens · nanoparticles · polymorphism · semiconductors · solid-state structures

[1] a) L. Corliss, N. Elliott, J. Hastings, *Phys. Rev.* **1956**, *104*, 924; b) C. N. R. Rao, K. P. R. Pishardy, *Prog. Solid State Chem.* **1976**, *10*, 207.
[2] a) N. Samarth, P. Klosowski, H. Luo, G. Geibultowicz, J. K. Furdyna, J. J. Rhyne, B. E. Larson, N. Otsuka, *Phys. Rev. B* **1991**, *44*, 4701; b) T. M. Giebultowicz, N. Samarth, H. Luo, J. K. Furdyna, P. Klosowski, J. J. Rhyne, *Phys. Rev. B* **1992**, *46*, 12076.
[3] J. K. Furdyna, *J. Appl. Phys.* **1988**, *64*, R29.
[4] P. R. Bressler, T. Klopper, H. E. Gumlich, *J. Vac. Sci. Technol. B* **1993**, *11*, 1621.
[5] M. E. Schlesinger, *J. Phase Equilib.* **1998**, *19*, 588.
[6] R. Lindsay, *Phys. Rev.* **1951**, *84*, 569.
[7] V. Thanigaimani, M. A. Angahi, *Thin Solid Films* **1994**, *245*, 146.
[8] a) S. Lei, T. Tang, H. Zheng, *Mater. Lett.* **2006**, *60*, 1625; b) H. J. Chun, J. Y. Lee, D. S. Kim, S. W. Yoon, J. H. Kang, J. Park, *J. Phys. Chem. C* **2007**, *111*, 519; c) D. S. Wang, W. Zheng, C. H. Hao, Q. Peng, Y. D. Li, *Chem. Eur. J.* **2009**, *15*, 1870.
[9] D. Litvinov, D. Gerthsen, A. Rosenauer, B. Daniel, M. Hetterich, *Appl. Phys. Lett.* **2004**, *85*, 751.
[10] R. M. Murray, B. C. Forbes, R. D. Heyding, *Can. J. Chem.* **1972**, *50*, 4059.
[11] S. H. Wei, A. Zunger, *Phys. Rev. B* **1993**, *48*, 6111.
[12] S. Kan, I. Felner, U. Banin, *Isr. J. Chem.* **2001**, *41*, 55.
[13] I. Ishibe, Y. Nabetani, T. Kato, T. Matsumoto, *J. Cryst. Growth* **2000**, *214/215*, 172.
[14] a) M. Okajima, T. Tohda, *J. Cryst. Growth* **1992**, *117*, 810; b) Y. Zhang, H. Wang, B. Wang, H. Yan, M. Yoshimura, *J. Cryst. Growth* **2002**, *243*, 214.
[15] T. Ito, K. Ito, M. Oka, *Jpn. J. Appl. Phys.* **1978**, *17*, 371.

